Pomegranate peel-derived exosome-like nanoparticles: A discarded treasure trove for colorectal cancer treatment

YIFEI DONG[1*], QIN YUAN[2*], CHAO CHEN[3] and ZHENG ZHANG[4]

[1]Department of Laboratory, The Eighth Hospital of Wuhan, Wuhan, Hubei 430012, P.R. China;
[2]Department of Oncology Medicine, Hubei Aerospace Hospital, Xiaogan, Hubei 432000, P.R. China ;
[3] Department of Anorectal Surgery, The Eighth Hospital of Wuhan, Wuhan, Hubei 430012, P.R. China;
[4]Department of Hepatobiliary, Pancreatic and Vascular Surgery, Hankou Hospital, Wuhan, Hubei 430012, P.R. China

Received October 15, 2025; Accepted February 16, 2026

DOI: 10.3892/ol.2026.15546

Abstract. Colorectal cancer (CRC) is the leading cause of cancer-related deaths. Thus, there is an urgent need for effective treatment strategies. Exosomes and exosome-like nanoparticles (ELNs) have recently received widespread attention due to their various bioactivity functions and potential clinical applications. The present study focused on the molecular mechanism of pomegranate peel-derived ELNs (PELNs) in anti-CRC therapy. PELNs were successfully extracted via the ultra-centrifugation method and were effectively received by CRC cells (SW480). In addition, the proliferation and migration of CRC cells treated with PELNs were significantly inhibited *in vitro*. RNA sequencing results indicated that PELN treatment affected the expression levels of numerous genes associated with signal transduction, cell cycle and cancer, suggesting its potential in the field of anti-CRC through crossing-kingdom regulation.

Introduction

Colorectal cancer (CRC) is the second leading cause of cancer-related mortality and a major global health burden (1). Epidemiological data show that the incidence of CRC is steadily rising, especially among young individuals (2). Although the latest advances in screening modes and therapeutic interventions, including immune checkpoint inhibitors and molecular targeted drugs, have improved clinical outcomes, metastatic CRC continues to pose significant treatment challenges. Treatment resistance development and early metastasis remain the key obstacles, leading to a 5-year survival of <15% for stage IV patients (3). This clinical reality highlights the pressing need to explore innovative, safer, and more effective treatment strategies for CRC.

Exosomes are nanovesicles with a lipid bilayer membrane structure. They are released by almost all cell types. Exosomes are rich in bioactive substances, such as nucleic acids, lipids and proteins (4), which play an important role in intercellular transmission, information exchange and immune regulation (5). Plant-derived exosome-like nanoparticles (ELNs) have attracted more attention in the fields of anti-inflammatory, antitumor and radioprotective effects as a result of their low immunogenicity, favorable biocompatibility, stability and biosafety (6). In addition, *Lycium ruthenicum Murray*-derived ELNs hinder Aβ-induced apoptosis of HT22 cells and reduce oxidative stress levels by activating the Nrf2/HO-1/NQO1 signaling pathway (7). *Polygonum multiflorum*-derived ELNs significantly inhibit proliferation and migration of liver cancer cells (8) and exert anti-photoaging effects by reducing ultraviolet-induced oxidative stress and promoting collagen formation (9). *Atractylodes macrocephala*-derived ELNs significantly improve ulcerative colitis by remodeling gut microbiota balance, modulating tryptophan metabolism, and suppressing the Th17 cell differentiation pathway (10). *Gardenia*-derived ELNs alleviate Parkinson's disease progression by attenuating dopaminergic neuronal apoptosis and inhibiting the p38 MAPK/p53 signaling pathway (11). Pomegranate vesicle extracts have been shown to prevent intestinal barrier dysfunction and liver injury/fibrosis in a mouse model of metabolic dysfunction-associated steatotic liver disease (12).

Pomegranate [*Punica granatum Linn* (*Punica granatum L.*)] is a highly nutritious fruit that has attracted considerable attention due to its notable pharmacological properties. The edible pomegranate flesh contains abundant bioactive compounds, including anthocyanins and ellagitannins, which have powerful antioxidant and vasculoprotective effects (13). The non-edible pomegranate peel accounts for ~40% of the total fruit weight and is typically discarded as agricultural waste. However, it has been found to contain beneficial active substances. It has

Correspondence to: Mr. Zheng Zhang, Department of Hepatobiliary, Pancreatic and Vascular Surgery, Hankou Hospital, 7 Erqi Side Road, Jiang'an, Wuhan, Hubei 430012, P.R. China
E-mail: 13477988786@163.com

Ms. Qin Yuan, Department of Oncology Medicine, Hubei Aerospace Hospital, 36 Beijing Road, Xiaogan, Hubei 432000, P.R. China
E-mail: waxhj20235754@qq.com

*Contributed equally

Key words: pomegranate peel, exosome-like nanoparticles, traditional Chinese medicine, colorectal cancer, cancer intervention

been indicated that the levels of antioxidant components and activities in pomegranate peel are markedly higher than in the seeds and pulp (14). Pomegranate-derived ELNs have shown significant anticancer effects against lung, breast and skin cancers (15). However, the effect of pomegranate peel-derived nanovesicles on CRC cells remains unexplored.

The present study explored the intervention mechanism of CRC with a focus on pomegranate peel-derived ELNs (PELNs). Differential ultra-centrifugation was successfully utilized for the first time to isolate and purify PELNs from the pericarp of *Punica granatum L*. A series of functional experiments was subsequently carried out *in vitro*, including cell internalization, proliferation, apoptosis and migration. Transcriptome sequencing experiment was then conducted to analyze the anti-CRC mechanism of PELNs.

Materials and methods

PELN isolation. ELNs were isolated from the juice found in the pomegranate peel. A total of ~50 g of pomegranate peel was washed with ultra-pure water, ground with phosphate-buffered saline (PBS) buffer, and filtered through a strainer to collect the leaching filtrate solution. The filtrate was then centrifuged at 500 x g for 10 min, 2,000 x g for 20 min, and 12,000 x g for 60 min to remove dead cells and cell debris (Fig. 1A). The supernatant was subsequently ultra-centrifuged at 100,000 x g for 70 min at 4˚C (Thermo Fisher Scientific, Inc.). The pellet was resuspended in PBS and then ultra-centrifuged again for 70 min. Finally, the PELNs were resuspended in PBS and stored at -80˚C until further analysis.

PELN characterization. PELN size and concentration were measured using a Nanoparticle Tracking Analysis (NTA) instrument (ZetaView; Particle Metrix GmbH). PELNs were then stained with 2% uranyl acetate for 1 min at room temperature, and images of their morphology structure were captured using transmission electron microscopy (TEM; Hitachi HT-7700; JEOL, Ltd.).

Cell culture. The CRC cell line SW480 utilized in the present study was obtained from Procell Life Science & Technology Co., Ltd. SW480 cells were cultured in Dulbecco's Modified Eagle medium (DMEM; Invitrogen; Thermo Fisher Scientific, Inc.) with 10% fetal bovine serum (FBS; HyClone™; Cytiva) and 1% penicillin/streptomycin (PS) solution in a 37˚C cell culture incubator with 5% CO_2.

Cell internalization. Next, 50 μl of PELNs was mixed with 4 μl of PKH26 red fluorescent cell membrane dye (MilliporeSigma) in 2 ml of PBS. The mixture was incubated at room temperature for 5 min and 2 ml of FBS was added to stop the staining reaction. The mixtures were subsequently ultra-centrifuged at 100,000 x g for 70 min at 4˚C. The pellet was re-suspended in PBS buffer and then ultra-centrifuged again for 70 min. Finally, the PKH26-labeled PELNs were re-suspended in PBS for future analysis.

SW480 cells were seeded in 24-well plates and treated with PKH26-labeled PELNs for 5 h. The cells were then fixed with 4% paraformaldehyde for 15 min at room temperature, stained with DAPI blue-fluorescent dye for 15 min at room temperature, and images were captured using confocal microscopy (TCS SP8; Leica Microsystems GmbH).

Cell proliferation assay. The effect of PELNs on SW480 cell proliferation was assessed using a Cell Counting Kit-8 (CCK-8; Beijing Solarbio Science & Technology Co., Ltd.). SW480 cells were seeded in 96-well plates and treated with PBS (Control group) or PELNs (PELN group) for 0, 24, 48 and 72 h. Next, 10 μl of CCK-8 reagent was added to each well and further cultured for 1 h at 37˚C. The absorbance was measured at 450 nm using an enzymatic reader (Bio-Rad Laboratories, Inc.).

Colony formation assay. SW480 cells were seeded in 6-well plates and treated with PBS or PELNs. After 14 days, cells were fixed with 4% paraformaldehyde for 15 min at room temperature and stained with crystal violet staining solution (cat. no. C0121; Beyotime Biotechnology) for 15 min at room temperature. The areas of cell colony formation were quantified using ImageJ software (v1.46r; National Institutes of Health).

Flow cytometric analysis of apoptosis. SW480 cells were seeded in 6-well plates and treated with PBS or PELNs. The cells were harvested using trypsin upon reaching 80% confluency, resuspended in PBS, and stained with 5 μl of Annexin V-FITC and 5 μl of propidium iodide (PI; Beijing Solarbio Science & Technology Co., Ltd.) for 15 min in the dark. Apoptotic cells were then quantified using a flow cytometer (MoFLO XDP; Beckman Coulter, Inc.) and CytExpert software (v2.3.1.22; Beckman Coulter, Inc.).

Wound healing assay. SW480 cells were seeded in 6-well plates until reaching 90% confluency. Then, straight scratches were made in each well using a 1-ml sterile pipette tip. After removing cell debris with a PBS wash, cells were cultured for 0, 24, or 48 h in 2 ml of DMEM with 1% FBS and 1% PS solution, containing PBS or PELNs ($1.0x10^9$ particles/ml), at 37˚C in a 5% CO_2 incubator. Wound healing was observed using a light microscope (bright-field). The migration distance was quantified by measuring the wound width using ImageJ software.

Transwell migration assay. SW480 cells were seeded in the upper chamber of a 24-well Transwell plate in 200 μl of DMEM containing PBS or PELNs. The lower chamber was filled with 500 μl of DMEM supplemented with 10% FBS and 1% penicillin/streptomycin. Cells were fixed with 4% paraformaldehyde for 15 min at room temperature after treatment for 24 h and stained with crystal violet staining solution (cat. no. C0121; Beyotime Biotechnology) for 15 min. The areas of cell migration were quantified using ImageJ software.

RNA extraction. The total RNA samples from SW480 cells treated with PBS or PELNs were extracted using TRIzol reagent (Invitrogen; Thermo Fisher Scientific, Inc.). TRIzol reagent was added to the sample, and the mixture was incubated for 5 min and mixed with chloroform, phenol, and isopropanol for 3 min according to the manufacturer instructions. The RNA

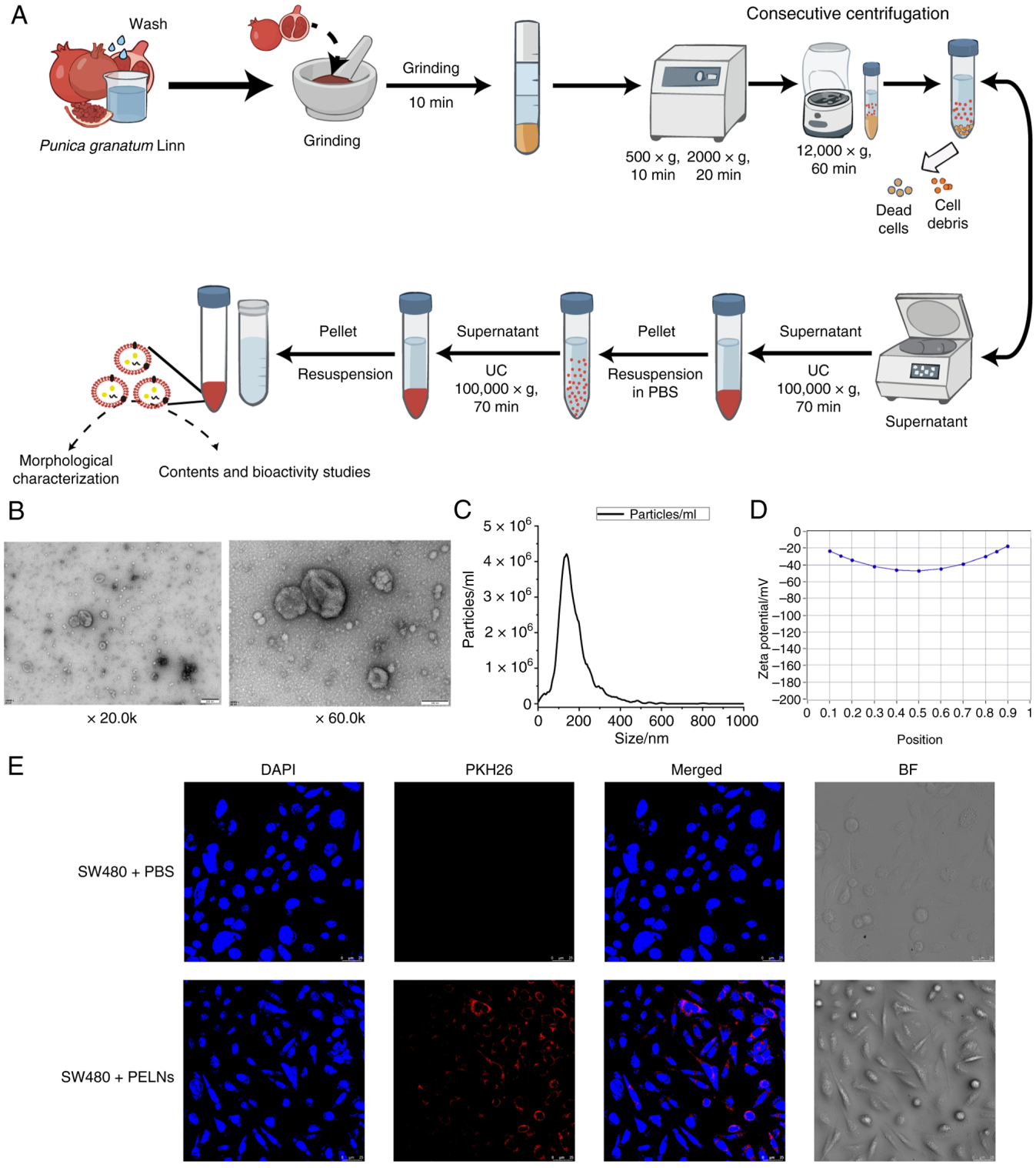

Figure 1. Isolation, characterization and cellular internalization of PELNs. (A) Schematic diagram of the preparation process for isolating PELNs from the peel of *Punica granatum*. (B) Representative transmission electron microscopy image of PELNs. Scale bar, 200 nm (left); 100 nm (right). (C) PELN concentration and size distribution. (D) Zeta potential distribution of PELNs. (E) PKH26-labeled PELNs (red) were received by SW480 cells [nuclei stained by DAPI (blue)]. Scale bar, 25 μm. PELNs, pomegranate peel-derived exosome-like nanoparticles; UC, ultracentrifugation; PBS, phosphate-buffered saline.

samples were collected with DEPC water by centrifugation at 12,000 x g for 15 min at 4˚C. RNA quality was assessed prior to library construction. Purity and concentration were measured using a NanoDrop spectrophotometer (Thermo Fisher Scientific, Inc.) and a Qubit 4.0 fluorometer (Thermo Fisher Scientific, Inc.), with a 260/280 nm ratio >1.8 required for sample acceptance. The integrity and quantity of the extracted RNA were measured using the Agilent 2100 system (Agilent Technologies, Inc.).

Transcriptome sequencing and analysis. The SW480 cells were seeded in 6-well plates and treated with PELNs or PBS

for 24 h for RNA-sequencing (RNA-Seq) analysis. Total RNA was extracted from the CRC cell samples, and mRNA was purified using the HieffNGS® mRNA isolation master kit (cat. no. 12603; Shanghai Yeasen Biotechnology Co., Ltd.). First-strand cDNA was synthesized using random hexamers, followed by second-strand synthesis with DNA polymerase I and RNase H. Double-stranded cDNA was end-repaired, adenylated, and ligated to sequencing adaptors. For purification and fragment selection, Hieff NGS® DNA Selection Beads (cat. no. 12601ES56; Yeasen Biotechnology Co., Ltd.) were used. After adapter ligation, bead-based size selection was performed using 0.6x and 0.2x ratios to enrich for fragments of the desired size. The final libraries were purified using a 0.8 x bead ratio and subsequently amplified by PCR. The purified libraries were quantified using a Qubit fluorometer (Thermo Fisher Scientific, Inc.) and initially measured in ng/μl. The molar concentration was then calculated based on the average fragment size determined by an Agilent 2100 system (Agilent Technologies, Inc.). Library circularization was performed using the MGIEasy Dual Barcode Circularization Module (cat. no. A0508; MGI Tech Co., Ltd.) prior to sequencing. Finally, the libraries were sequenced on the DNBSEQ-T7 platform (MGI Tech Co., Ltd.) using the DNBSEQ-T7RS High-throughput Sequencing Set (App-D FCL PE150, V3.0; cat. no. Group 100-000016-00; MGI Tech Co., Ltd.) in paired-end 150 bp (PE150) mode, following the manufacturer's instructions.

StringTie (v2.1.5; http://ccb.jhu.edu/software/stringtie/index.shtml) was used to compare the read count values for each gene as the original expression level. Fragments per kilobase of transcript per million mapped reads were then utilized to standardize the expression. Differentially expressed genes (DEGs) were then analyzed using DESeq2 (v1.30.1; https://bioconductor.org/packages//release/bioc/html/DESeq2.html), with screening conditions set as follows: $|\log_2 \text{FoldChange}| > 1$ and adjusted P-value (padj) ≤ 0.05. Kyoto Encyclopedia of Genes and Genomes (KEGG) and Gene Ontology (GO) enrichment analyses of DEGs were performed using clusterProfiler (v3.8.1; https://github.com/GuangchuangYu/clusterProfiler). Significant enrichment results (P-adj ≤ 0.05) were selected to identify connections between genes and pathways.

Statistical analysis. Statistical significance was analyzed using GraphPad Prism 5.0 (Dotmatics) and Microsoft Excel (2010) software. All data are presented as the mean ± standard deviation (mean ± SD). Paired Student's t-test was performed to compare the means of two data sets. $P<0.05$ was considered to indicate a statistically significant difference.

Results

Isolation, characterization and cellular internalization of PELNs. PELNs were isolated and purified from *Punica granatum L*. using filtration and differential ultra-centrifugation (Fig. 1A). TEM analysis revealed that the isolated particles exhibited a cup-shaped nanostructure with exosome-like characteristics (Fig. 1B). NTA analysis revealed that PELNs had an average diameter of 152.0 nm, a concentration of $4.2x10^{10}$ particles/ml, and a zeta potential of -26.14 mV (Fig. 1C and D).

An internalization experiment was carried out to investigate the biological function of PELNs in the anti-CRC mechanism. After treating SW480 cells with PKH26-labeled PELNs or PBS, red fluorescence was only observed in the PELN-treated group and located around the blue fluorescence, but not in the control group (Fig. 1E). These results indicated that PELNs were effectively received by the CRC cells.

PELNs inhibit CRC cell proliferation and induce apoptosis. CCK-8 and colony formation assays were performed to further evaluate the effect of PELNs on CRC cell proliferation. The proliferation ability of CRC cells treated with PELNs for 24, 48 and 72 h was significantly reduced compared with that of the control group ($P<0.001$; Fig. 2A and B). In the colony formation assay, the areas of SW480 cells stained with crystal violet in the PELN group were significantly decreased ($P<0.01$; Fig. 2C and D).

Furthermore, SW480 cells were treated with PELNs for 24 h to investigate whether PELNs affect CRC cell apoptosis. Early and late apoptotic cells were labeled with Annexin V-FITC/PI. Flow cytometric analysis indicated that the PELN treatment significantly increased the rate of CRC cell apoptosis ($P<0.01$; Fig. 2E and F).

PELNs inhibit CRC cell migration. Wound healing and Transwell migration assays were carried out to evaluate the effect of PELNs on the migration ability of CRC cells. SW480 cells were treated with PELNs after generating scratch wounds in the plate wells. The changes in wound width were observed at 0, 24 and 48 h. The wound width in the PELN-treated group was significantly increased compared with that in the control group ($P<0.001$; Fig. 3A and B).

SW480 cells were incubated with PELNs in the upper chamber of Transwell plates for 24 h. The migratory cells were then quantified. Crystal violet-stained areas in the PELN group demonstrated a significant reduction ($P<0.05$; Fig. 3C and D). These results indicated that PELNs significantly inhibit CRC cell migration *in vitro*.

Transcriptomic analysis of PELN-treated CRC cells. The sample correlation analysis heat map indicated that the correlation between repeated samples was strong, confirming experimental reproducibility (Fig. 4A). DEGs of SW480 cells after treatment with PBS (Control-1, Control-2 and Control-3) or PELNs (PELNs-1, PELNs-2 and PELNs-3) were statistically analyzed. The results of a volcano plot and cluster analysis showed that there were 2,303 upregulated and 3,295 downregulated genes (Fig. 4B and C). KEGG pathways and GO terms related to DEGs were subsequently analyzed based on the functional annotation results in the database.

Statistical analysis of KEGG pathway enrichment (top 20) indicated that multiple enriched pathways were associated with signal transduction and cancer, including 'MAPK signaling pathway' (ID: map04010), 'Hippo signaling pathway' (ID: map04390), 'NF-kappa B signaling pathway' (ID: 04064), 'TNF signaling pathway' (ID: map04668), 'Wnt signaling pathway' (ID: map04310), 'Estrogen signaling pathway' (ID: map04915), 'Cellular senescence' (ID: map04218), 'p53 signaling pathway' (ID: map04115), 'Cell cycle' (ID:

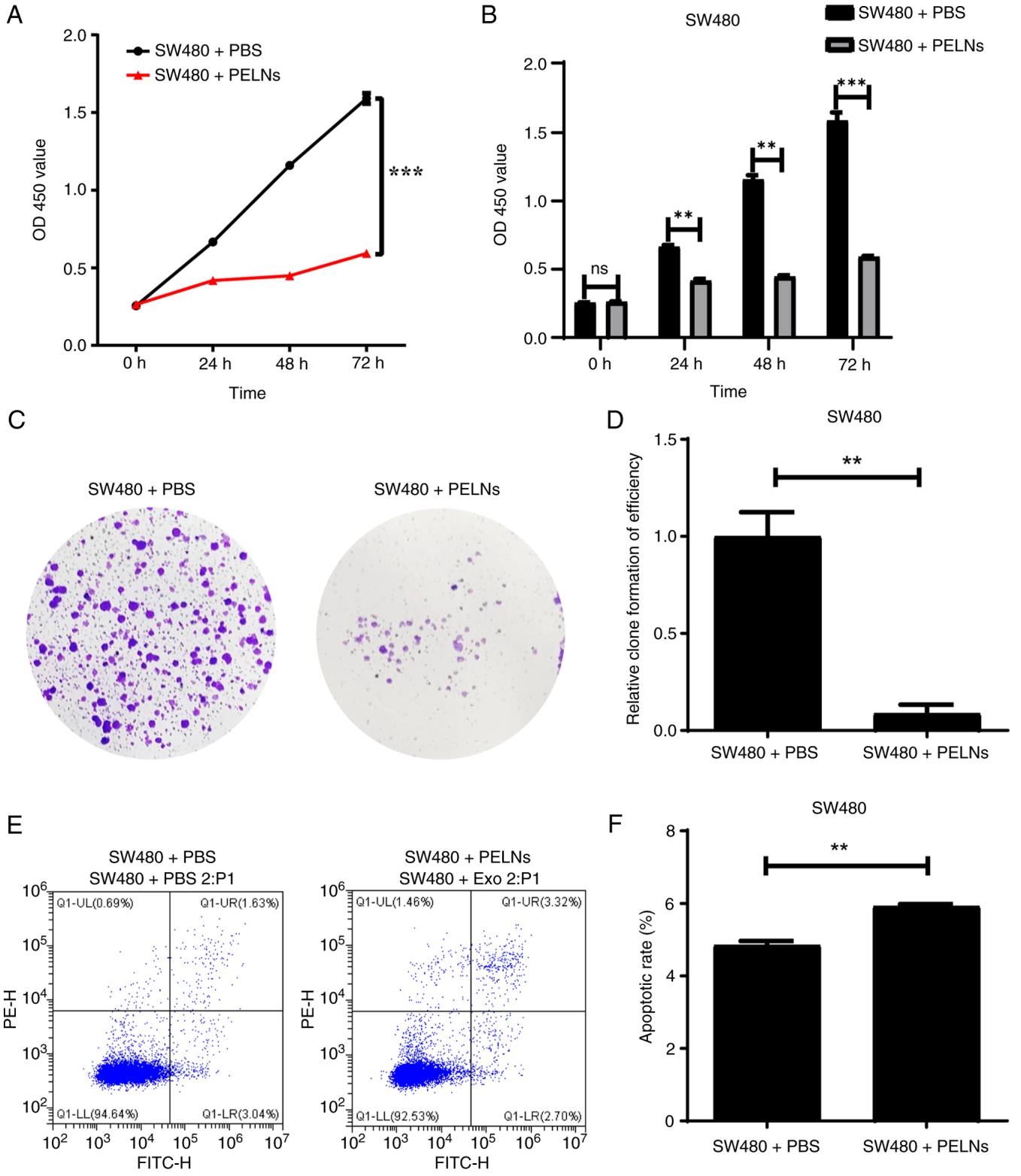

Figure 2. Proliferation and apoptosis of SW480 cells after treatment with PELNs. (A and B) Schematic and quantitative diagrams of proliferation of SW480 cells treated with PBS or PELNs. Data are presented as the mean ± SD (n=5). (C and D) Schematic and quantitative diagrams of clone formation of SW480 cells treated with PBS or PELNs. Data are presented as the mean ± SD (n=3). (E and F) Schematic and quantitative diagrams of flow cytometric analysis of SW480 cell apoptosis treated with PBS or PELNs. Data are presented as the mean ± SD (n=3). **P<0.01 and ***P<0.001. PELNs, pomegranate peel-derived exosome-like nanoparticles; PBS, phosphate-buffered saline; ns, not significant.

map04110), 'FoxO signaling pathway' (ID: map04068), 'ECM-receptor interaction' (ID: map04512), 'MicroRNAs in cancer' (ID: map05206) and 'Transcriptional misregulation in cancer' (ID: map05202) (Fig. 4D, Table SI).

GO enrichment analysis of the top 20 molecular function terms demonstrated significant enrichment for processes directly related to cell cycle regulation and signal transduction, including 'MAP kinase tyrosine/serine/threonine

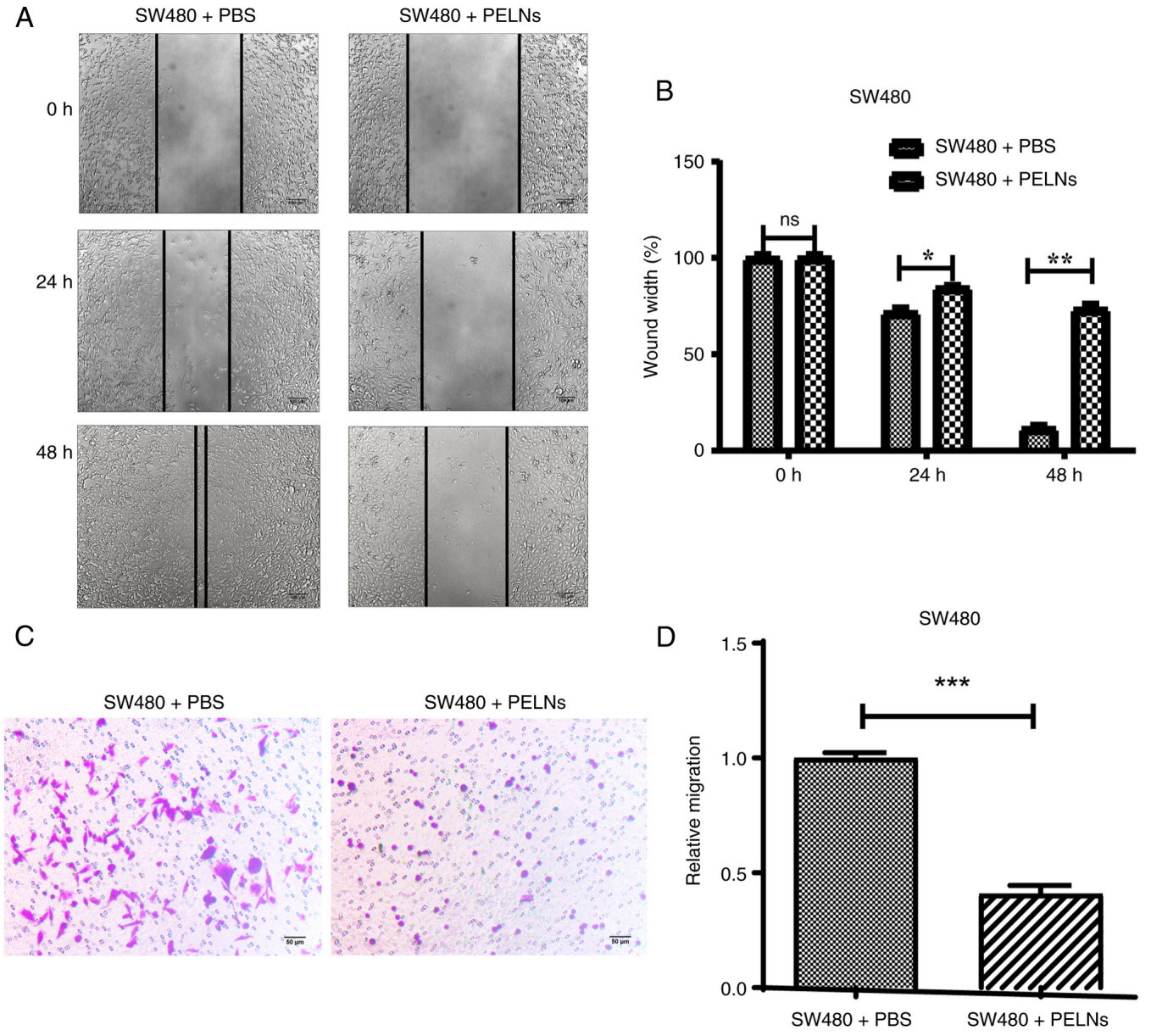

Figure 3. SW480 cell migration after treatment with PELNs. (A and B) Schematic and quantitative diagrams of wound healing of SW480 cells treated with PBS or PELNs. (C and D) Schematic and quantitative diagrams of Transwell migration of SW480 cells treated with PBS or PELNs. Data are presented as the mean ± SD (n=3). *P<0.05, **P<0.01 and ***P<0.001. PELNs, pomegranate peel-derived exosome-like nanoparticles; PBS, phosphate-buffered saline; ns, not significant.

phosphatase activity' (GO: 0017017), 'protein kinase activity' (GO: 0004672), 'protein serine/threonine kinase activity' (GO: 0004674), 'DNA replication' (GO: 0006260), 'protein phosphorylation' (GO: 0006468), 'signal transduction' (GO: 0007165), 'signaling receptor binding' (GO: 0005102), and 'DNA replication initiation' (GO: 0006270) (Fig. 4E, Table SII). Transcriptome sequencing analysis results indicated that the DEGs associated with PELNs specifically affected the proliferation and migration abilities of CRC cells.

Discussion

Exosomes were considered cellular metabolism waste in 1983 (16,17). Thorough research studies gradually discovered that exosomes have specific cup-shaped nanovesicle structures and that they participate in cellular information exchange, tumor occurrence and development, and wound healing physiological and pathological processes. PELN advantages include source abundance, low immunogenicity and high biocompatibility. PELNs have demonstrated significant potential in medical applications due to their anti-inflammatory properties (balloon flower root ELNs) (18), antitumor effects (garlic ELNs) (19) and osteoporosis' prevention capacity (yam ELNs) (20). Pomegranate peel is discarded as waste in daily life, but it is commonly used as a traditional Chinese medicine for antimicrobial (21), antioxidant (22) and wound healing needs (23). However, the inhibitory effect of pomegranate PELNs on cancer has not been explored. The present study for the first time, to the best of our knowledge, successfully isolated high concentrations of ELNs from the peel of *Punica granatum L*. Functional experiments identified that PELNs inhibit the proliferation and migration of CRC cells.

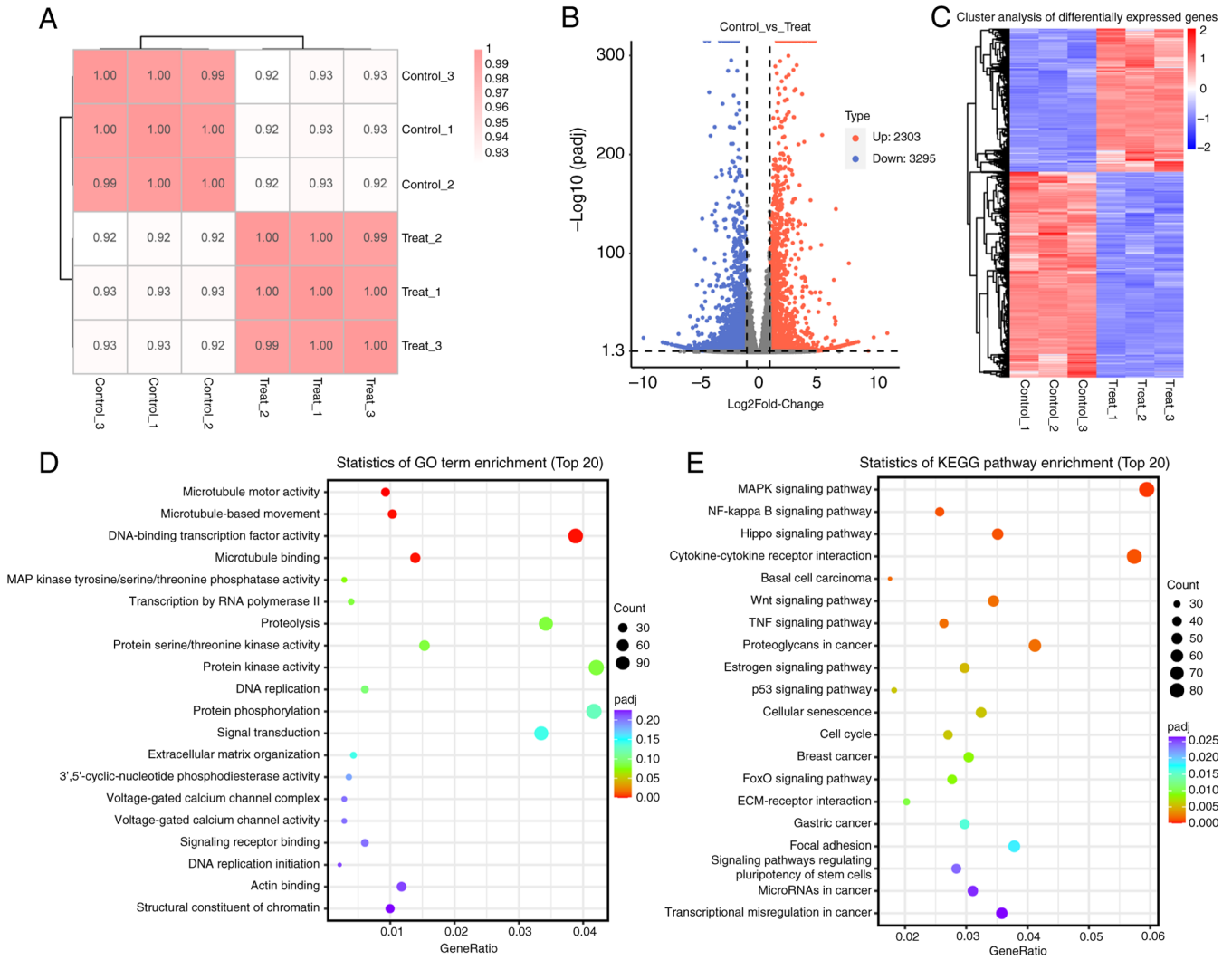

Figure 4. Anti-colorectal cancer molecular mechanism of PELNs. (A) Sample correlation analysis heat map. (B and C) Volcano plot map and cluster analysis diagram of differentially expressed genes in SW480 cells treated with phosphate-buffered saline or PELNs. (D and E) Balloon plots of KEGG pathway (top 20) and GO term enrichment (top 20) analyses. PELNs, pomegranate peel-derived exosome-like nanoparticles; KEGG, Kyoto Encyclopedia of Genes and Genomes; GO, Gene Ontology.

KEGG and GO analyses of RNA-Seq revealed that PELNs inhibited cancer-associated pathways, including the MAPK, Hippo, NF-kappa B and Wnt signaling pathways. Pellino 2 is an E3 ubiquitin ligase that regulates the CRC cell cycle, apoptotic signals, and downstream epithelial-mesenchymal transition program via the MAPK signaling pathway (24). In addition, Sakuma *et al* (25) demonstrated that overexpression of heterogeneous nuclear ribonucleoprotein L-like upregulated the expression levels of PCNA, RFC3 and FEN1, promoted cell cycle progression, and thereby enhanced CRC cell proliferation. PELNs may play an anti-CRC role by downregulating the expression of DNA replication initiation promoter genes PCNA and FEN1 (Table SIII) and disrupting normal DNA repair and cell cycle in SW480 cells. The canonical Wnt signaling pathway depends on the β-catenin protein to regulate gene expression, cell migration, proliferation and differentiation during the pathological development of CRC (26). Zheng *et al* (27) reported that as a therapeutic target for CRC, LDL receptor related protein 2 (LRP2) enhances GSK3β/β-catenin signaling to promote CRC metastasis. In the present study, DEG LRP2 was significantly downregulated (Table SIII) after treatment with PELNs, which may be the main reason for PELN SW480 cell migration inhibition. In summary, the molecular mechanism by which PELNs restrained CRC progression may primarily have acted through the MAPK/Wnt signaling pathway and cell cycle regulation.

The primary limitation of the present study is that the specific composition of PELNs remains unclarified. Accumulating evidence indicates that ELNs carry abundant microRNAs (miRNAs or miRs) (28), proteins (29), lipids (30) and metabolites (31). It has been reported that pomegranate-ELNs are enriched with proteins including chitinase, lipid transfer protein and chalcone synthase (12). Pomegranate-ELNs are effective in improving pancreatitis and preventing metabolic dysfunction-associated fatty liver disease (32). *Centella Asiatica*-ELNs are enriched with miRNAs (for example, aof-miR159, fve-miR396c-3p and aof-miR396b), lipid components (for example, ceramide, triglyceride and, hexosyl-ceramide), and numerous proteins involved in key biological processes (33). The miR-7972

abundant in *Rehmanniae* Radix-ELNs is an active component responsible for the anti-inflammatory activity of the fresh plant (34). *Momordica charantia*-ELNs, which are rich in metabolism-related proteins and anti-inflammatory and antioxidant lipid components, have demonstrated efficacy in treating diabetes and alleviating ulcerative colitis, with studies revealing that their therapeutic effects are mediated through the repair of insulin-secretory function and comprehensive renovation of the intestinal microenvironment (35,36). These precedents underscore that elucidating molecular cargo is the critical step linking observed phenotype to mechanistic understanding, thereby exemplifying the established 'phenotype, composition, mechanism' research paradigm applicable to ELNs studies. *In vitro* functional validation serves not only as the foundational core of such research but also provides critical direction and justification for subsequent in-depth compositional analysis. Consequently, the conclusive *in vitro* data presented in the present study confirm the potent anti-CRC bioactivity of PELNs. This provides a solid basis for further investigation and clearly delineates the future research trajectory of the current study. First, the particle-free supernatant will be used as a negative control to definitively attribute the observed anticancer effects to PELNs. Subsequently, integrated multi-omics analyses (for example, miRNA sequencing, proteomics and lipidomics) will be performed. These analyses will systematically identify the constituents of PELNs and pinpoint key bioactive molecules, such as specific miRNAs or functional proteins, to elucidate their anti-CRC mechanism of action. Finally, comprehensive *in vivo* studies on the biodistribution, safety and antitumor efficacy of PELNs will be conducted. Collectively, these studies are crucial for laying the practical groundwork for clinical translation and for advancing the role of plant-derived nanotherapeutics in CRC treatment.

Pomegranate PELNs are a natural biological nanomaterial that exhibit significant inhibitory effects on the proliferation and migration of CRC cells. This finding greatly enhanced the potential value of future research into the biological functions and clinical applications of plant-derived ELNs, fruit peel, and other 'neglected waste' materials. In addition, engineering modifications of PELNs, such as surface modification of targeted peptides or internal delivery of small molecule drugs, are expected to further enhance their anti-cancer effects. In the future, PELNs have great potential for precise targeted therapy of malignant tumors. Nevertheless, advancing PELNs to the clinic will require further validation of their composition, safety and *in vivo* efficacy.

Acknowledgements

The authors would like to thank Dr Zhan Leilei (Wuhan GeneCreate Biological Engineering Co., Ltd.) for critically discussing the manuscript.

Funding

The present study was supported by the Wuhan Traditional Chinese Medicine Scientific Research Project (grant no. WZ22C24; 2022-2024).

Availability of data and materials

The data generated in the present study may be found in the BioProject database under accession number PRJNA1307758 or at the following URL: https://www.ncbi.nlm.nih.gov/bioproject/?term=PRJNA1307758.

Authors' contributions

YD and QY conceived and designed the study, performed the experiments, and analyzed the data. ZZ and CC participated in the design of experiments, data analysis and data interpretation. All authors read and approved the final version of the manuscript. YD and QY confirm the authenticity of all the raw data.

Ethics approval and consent to participate

Not applicable.

Patient consent for publication

Not applicable.

Competing interests

The authors declare that they have no competing interests.

References

1. Bray F, Laversanne M, Sung H, Ferlay J, Siegel RL, Soerjomataram I and Jemal A: Global cancer statistics 2022: GLOBOCAN estimates of incidence and mortality worldwide for 36 cancers in 185 countries. CA Cancer J Clin 74: 229-263, 2024.
2. Siegel RL, Wagle NS, Cercek A, Smith RA and Jemal A: Colorectal cancer statistics, 2023. CA Cancer J Clin 73: 233-254, 2023.
3. Biller LH and Schrag D: Diagnosis and treatment of metastatic colorectal cancer: A review. JAMA 325: 669-685, 2021.
4. Isaac R, Reis FCG, Ying W and Olefsky JM: Exosomes as mediators of intercellular crosstalk in metabolism. Cell Metab 33: 1744-1762, 2021.
5. Chen Q, Li Q, Liang Y, Zu M, Chen N, Canup BSB, Luo L, Wang C, Zeng L and Xiao B: *Natural exosome*-like nanovesicles from edible tea flowers suppress metastatic breast cancer via ROS generation and microbiota modulation. Acta Pharm Sin B 12: 907-923, 2022.
6. Ling Y, Li X, Gao H, Liu Y, Liu Y, Zheng J, Zhu J, Zhao C, Shi Y, Lu J and Yi J: Biyang floral mushroom-derived exosome-like nanovesicles: Characterization, absorption stability and ionizing radiation protection. Food Funct 15: 6900-6913, 2024.
7. Zhang Y, Lu L, Li Y, Liu H, Zhou W and Zhang L: Response surface methodology optimization of Exosome-like nanovesicles extraction from *Lyceum ruthenicum* murray and their inhibitory effects on Aβ-Induced apoptosis and oxidative stress in HT22 cells. Foods 13: 3328, 2024.
8. Yang M, Xu L and Wang W: Molecular anti-tumorigenic mechanism of Radix *Polygoni Multiflori*-derived exosome-like nanoparticles. Heliyon 11: e41918, 2025.
9. He J, Fu L, Shen Y, Teng Y, Huang Y, Ding X, Xu D, Cui H, Zhu M, Xie J, *et al*: *Polygonum multiflorum* extracellular Vesicle-Like nanovesicle for skin photoaging therapy. Biomater Res 28: 0098, 2024.
10. Tan X, Gao B, Xu Y, Zhao Q, Jiang J, Sun D, Zhang Y, Zhou S, Fan JB, Zhang M and Zhao K: *Atractylodes macrocephala*-derived extracellular vesicles-like particles enhance the recovery of ulcerative colitis by remodeling intestinal microecological balance. J Nanobiotechnology 23: 433, 2025.
11. Chen W, Wang H, Ye X, Hao X, Yan F, Wu J, Li D, Wang Y and Xu L: *Gardenia*-derived extracellular vesicles exert therapeutic effects on dopaminergic neuron apoptosis-mediated Parkinson's disease. NPJ Parkinsons Dis 11: 200, 2025.

12. Kim JS, Song BJ and Cho YE: Pomegranate-derived Exosome-like nanovesicles containing ellagic acid alleviate gut leakage and liver injury in MASLD. Food Sci Nutr 13: e70088, 2025.
13. Wang D, Özen C, Abu-Reidah IM, Chigurupati S, Patra JK, Horbanczuk JO, Jóźwik A, Tzvetkov NT, Uhrin P and Atanasov AG: Vasculoprotective effects of pomegranate (*Punica granatum* L.). Front Pharmacol 9: 544, 2018.
14. Mastrodi Salgado J, Ferreira TRB, De Oliveira Biazotto F and Dos Santos Dias CT: Increased antioxidant content in juice enriched with dried extract of pomegranate (*Punica granatum*) Peel. Plant Foods Hum Nutr 67: 39-43, 2012.
15. Sharma P, McClees SF and Afaq F: Pomegranate for prevention and treatment of cancer: An update. Molecules 22: 177, 2017.
16. Harding C, Heuser J and Stahl P: Receptor-mediated endocytosis of transferrin and recycling of the transferrin receptor in rat reticulocytes. J Cell Biol 97: 329-339, 1983.
17. Pan BT and Johnstone RM: Fate of the transferrin receptor during maturation of sheep reticulocytes in vitro: Selective externalization of the receptor. Cell 33: 967-978, 1983.
18. Kim M, Jang H and Park JH: Balloon flower Root-derived extracellular vesicles: In vitro assessment of Anti-Inflammatory, proliferative, and antioxidant effects for chronic wound healing. Antioxidants (Basel) 12: 1146, 2023.
19. Xu J, Yu Y, Zhang Y, Dai H, Yang Q, Wang B, Ma Q, Chen Y, Xu F, Shi X, *et al*: Oral administration of garlic-derived nanoparticles improves cancer immunotherapy by inducing intestinal IFNγ-producing γδ T cells. Nat Nanotechnol 19: 1569-1578, 2024.
20. Hwang JH, Park YS, Kim HS, Kim DH, Lee SH, Lee CH, Lee SH, Kim JE, Lee S, Kim HM, *et al*: Yam-derived exosome-like nanovesicles stimulate osteoblast formation and prevent osteoporosis in mice. J Control Release 355: 184-198, 2023.
21. Abu-Niaaj LF, Al-Daghistani HI, Katampe I, Abu-Irmaileh B and Bustanji YK: Pomegranate Peel: Bioactivities as antimicrobial and cytotoxic agents. Food Sci Nutr 12: 2818-2832, 2024.
22. Zhai X, Zhu C, Zhang Y, Sun J, Alim A and Yang X: Chemical characteristics, antioxidant capacities and hepatoprotection of polysaccharides from pomegranate peel. Carbohydr Polym 202: 461-469, 2018.
23. Yan H, Peng KJ, Wang QL, Gu ZY, Lu YQ, Zhao J, Xu F, Liu YL, Tang Y, Deng FM, *et al*: Effect of pomegranate peel polyphenol gel on cutaneous wound healing in alloxan-induced diabetic rats. Chin Med J (Engl) 126: 1700-1706, 2013.
24. Liu J, Hu S, Zhao L, Yang Y, Wu G, Duan Y, Ma X, Wang P, Zhang Z and Zong H: PELI2 inhibits colorectal cancer development through MAPK signaling pathway. Mol Med 31: 235, 2025.
25. Sakuma K, Sasaki E, Kimura K, Komori K, Shimizu Y, Yatabe Y and Aoki M: HNRNPLL stabilizes mRNA for DNA replication proteins and promotes cell cycle progression in colorectal cancer cells. Cancer Sci 109: 2458-2468, 2018.
26. Cheng X, Xu X, Chen D, Zhao F and Wang W: Therapeutic potential of targeting the Wnt/β-catenin signaling pathway in colorectal cancer. Biomed Pharmacother 110: 473-481, 2019.
27. Zheng X, Liu H, Zhong X, Liu X, Cai Z, Chen Y, He X, Lan P and Wu X: LDL receptor related protein 2 to promote colorectal cancer metastasis via enhancing GSK3β/β-catenin signaling. J Clin Oncol 39: e15507, 2021.
28. Leng Y, Yang L, Pan S, Zhan L and Yuan F: Characterization of blueberry exosome-like nanoparticles and miRNAs with potential cross-kingdom human gene targets. Food Sci Human Wellness 13: 869-878, 2024.
29. Sun J, Du L, Qu Z, Wang H, Dong S, Li X and Zhao H: Integrated metabolomics and proteomics analysis to study the changes in *Scutellaria baicalensis* at different growth stages. Food Chemistry 419: 136043, 2023.
30. Sui Y, Sun X, Liu Q, Qi G, Yang Y, Zhang X, Francis OB, Wang Y, Liu R, Li X, *et al*: Mori fructus-derived extracellular vesicle-like nanoparticles regulate dyslipidemia and prevent atherosclerosis progression via miRNAs. Phytomedicine 146: 157128, 2025.
31. Fu J, Liu Z, Feng Z, Huang J, Shi J, Wang K, Jiang X, Yang J, Ning Y, Lu F, *et al*: *Platycodon grandiflorum* exosome-like nanoparticles: The material basis of fresh *Platycodon grandiflorum* optimality and its mechanism in regulating acute lung injury. J Nanobiotechnol 23: 270, 2025.
32. Kang H, Hu Q, Yang Y, Huang G, Li J, Zhao X, Zhu L, Su H, Tang W and Wan M: Urolithin A's role in alleviating severe acute pancreatitis via endoplasmic Reticulum-mitochondrial calcium channel modulation. ACS Nano 18: 13885-13898, 2024.
33. Shi R, Tan W, Jin H, Chan SI, Li W, Lei SS, Cui G, Wang Y, Yang DH and Zhong Z: MicroRNA-enriched Plant-derived exosomes alleviate colitis by modulating systemic immunity, metabolic homeostasis, and *Gut microbiota*. Adv Sci (Weinh) 12: e05921, 2025.
34. Qiu FS, Wang JF, Guo MY, Li XJ, Shi CY, Wu F, Zhang HH, Ying HZ and Yu CH: Rgl-exomiR-7972, a novel plant Exosomal MicroRNA derived from fresh *Rehmanniae* radix, ameliorated lipopolysaccharide-induced acute lung injury and *Gut dysbiosis*. Biomed Pharmacother 165: 115007, 2023.
35. Han M, Wang J, Zhang Z, Yan Z, Wang Z, Guan X, Wang S, Mao Y and Zhang J: *Momordica Charantia* L.-derived extracellular vesicles achieve pancreatic-targeted delivery and repair insulin-secretory function through dual mechanisms via lymphatic transport. Chemical Engineering J 520: 165747, 2025.
36. Gao B, Huang X, Fu J, Chen L, Deng Z, Wang S, Zhu Y, Xu C, Zhang Y, Zhang M, *et al*: Oral administration of *Momordica charantia*-derived extracellular vesicles alleviates ulcerative colitis through comprehensive renovation of the intestinal microenvironment. J Nanobiotechnology 23: 261, 2025.